

Chapter 12

When Human Visual Performance Is Imperfect—How to Optimize the Collaboration Between One Human Operator and Multiple Field Robots

Hong Cai and Yasamin Mostofi

12.1 Introduction

In recent years, there have been great technological developments in robotics, in areas such as navigation, motion planning, and group coordination. However, while robots are becoming capable of more complicated tasks, there still exist many tasks which robots simply cannot perform to a satisfactory level when compared to humans. A complex visual task, such as recognition and classification in the presence of uncertainty, is one example of such tasks [2]. Thus, proper incorporation of human assistance will be very important to robotic missions.

More recently, the research community has been looking into the role of humans and different aspects of human–robot collaboration. In control and robotics, for instance, the Drift Diffusion Model from cognitive psychology [7, 14] has been heavily utilized in modeling human decision-making and the overall collaboration. Chipalkatty [8] shows how to incorporate human factors into a Model Predictive Control framework, in which human commands are predicted ahead of time. Utilizing machine learning, researchers have also looked into transferring human skills to robots [15] and incorporating human feedback to robot learning [12]. Several human–machine interfaces have been studied. Srivastava [13] has designed a Decision Support System considering the ergonomic factors of the human operator to optimize how the machine should provide information to the human operator. Branson et al. [2] propose a collaboration interface that resembles the 20-question game for bird classification. Experimental studies have been conducted on how humans and robots interact and cooperate in simulated scenarios, such as urban

H. Cai (✉) · Y. Mostofi
Department of Electrical and Computer Engineering, University of California,
Santa Barbara, CA, USA
e-mail: hcai@ece.ucsb.edu

Y. Mostofi
e-mail: ymostofi@ece.ucsb.edu

search and rescue operations [3, 10]. In [4–6], the fact that human visual performance is not perfect is taken into account in the collaboration between one human operator and a single field robot, emphasizing the importance of properly asking for human’s help. More specifically, in [4, 6] we showed how to predict human visual performance for the case where additive noise is the only source of uncertainty. In [5], we proposed an automated machine learning-based approach that allows the robot to probabilistically predict human visual performance for a visual input, with any source of uncertainty, and experimentally validated our approach.

In this chapter, we are interested in the optimization of the human–robot collaboration in visual tasks such that the strengths of both are properly combined in task planning and execution. We know that humans can do complex visual tasks, such as recognition and classification, in the presence of a high level of uncertainty, while robots can traverse harsh and potentially dangerous terrains. *Human visual performance, however, is not perfect as we established in [4, 5].* We thus incorporate a new paradigm, i.e., *when to ask humans for help* [4, 5], into the optimization of the collaboration between a human operator and *multiple robots*. In this approach, the collaboration properly takes advantage of the human’s superior visual performance and the robot’s exploration capability, while considering the fact that human visual performance is not perfect, allowing the robots to ask for help in an optimized manner. More specifically, consider a robotic field exploration and target classification task where the robots have limited onboard energy budgets and share a limited number of queries to the human operator. Due to these restrictions, the robots cannot query the human operator all the time for help with classification. On the other hand, they may not have sufficient resources or capabilities to explore the field (and reduce the sensing uncertainty) to the level that their own classification over the whole field becomes acceptable. In this chapter, we then show when the robots should ask the human for help, when they should rely on their own classification, and when they should further explore the environment by co-optimizing their motion, sensing, and communication with the human operator.

In order to solve such co-optimization problems, the robots only need to understand the extent of human visual capabilities and their own performance. For instance, a robot may collect data with a high level of uncertainty. Yet, the human may be able to make sense out of this data and perform an accurate classification of the target of interest. If a robot can properly understand this, it can then judge if it should stop sensing and present the data to the human, or if it should gather more sensing data. In Sect. 12.2, we summarize our previous work [4] on how to probabilistically predict human and robot visual performances when additive noise is the only source of uncertainty. In Sect. 12.3, we then show how to optimize the collaboration between one human operator and multiple field robots when a probabilistic metric of human visual performance is given. We mathematically characterize the optimal decisions that arise from our optimization framework. Based on numerical evaluations, we then verify the efficacy of our design in Sect. 12.4 and show that significant resource savings can be achieved.

The work presented in this chapter is an extension of our previous work [4] to a multi-robot setting. More specifically, in [4], we considered the fact that human

visual performance is not perfect in the collaboration of one robot and one human operator. We showed how to predict human visual performance for the case where additive noise is the main source of uncertainty. In this chapter, we extend [4] to a multiple robots setting, with an emphasis on mathematical analysis. More specifically, in this multi-robot setting, interesting new properties arise which we study both mathematically and numerically. We note that while this chapter uses the prediction of human visual performance from [4], a more realistic prediction of human visual performance from [5] can be incorporated in the numerical results as part of future work.

12.2 Human and Robot Performance in Target Classification [4]

In this section, we briefly summarize human and robot classification capabilities in the presence of additive noise based on our previous work [4]. Consider the case where the robot has discovered a target via taking a picture and needs to classify it based on a given set of target possibilities. For example, Fig. 12.1 (left) shows four possible images that are shown to the robot prior to the task. The sensing of the robot in the field, however, is in general subject to noise, low resolution, occlusion, and other uncertainties, which will degrade its classification accuracy. Figure 12.1 (right) shows a sample case where an image is corrupted by an additive Gaussian noise with variance of 2. If the robot could accurately model all the uncertainties and use the best detector accordingly, it would outperform the humans. This, however, is not possible in realistic scenarios as it is impossible for the robot to know/model every source of uncertainty or derive the optimal classifier due to the complexity of a real life visual task. This is why the robot can benefit from the collaboration with the human tremendously by properly taking advantage of human visual abilities. Human performance, however, is not perfect, which requires proper modeling.

In our previous work [4], human and robot performance curves were obtained for the following scenario. The robot takes an image in the field, which is corrupted by an additive Gaussian noise with a known variance but an unknown mean, and then undergoes a truncation process that is unknown to the robot. Figure 12.2 shows the performance curves of the human and the robot using noise variance as the metric. The solid line shows the true probability of correct classification of the robot using the minimum distance detector, which would have been the optimal detector under zero-mean additive Gaussian noise. The dashed line shows the human performance obtained from the data collected utilizing Amazon Mechanical Turk (MTurk). For instance, in Fig. 12.1 (right), humans can achieve an average probability of correct classification of 0.744, which is considerably higher than robot performance (0.5).

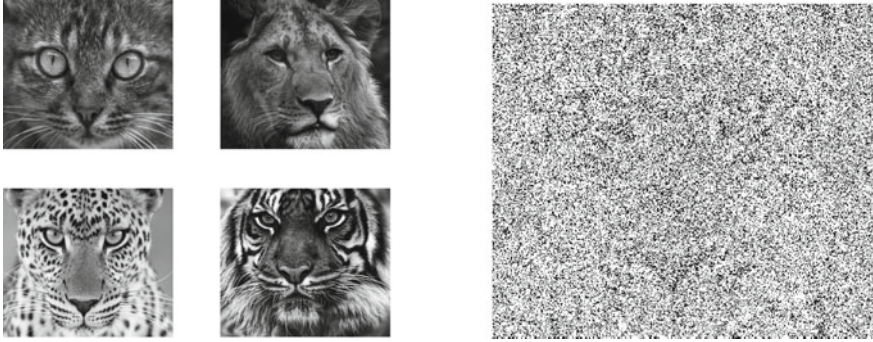


Fig. 12.1 (left) Gray-scale test images of cat, leopard, lion, and tiger used in our study [4]. (right) A sample corrupted image (leopard) with noise variance of 2 (© 2015 IEEE. Reprinted, with permission, from [4])

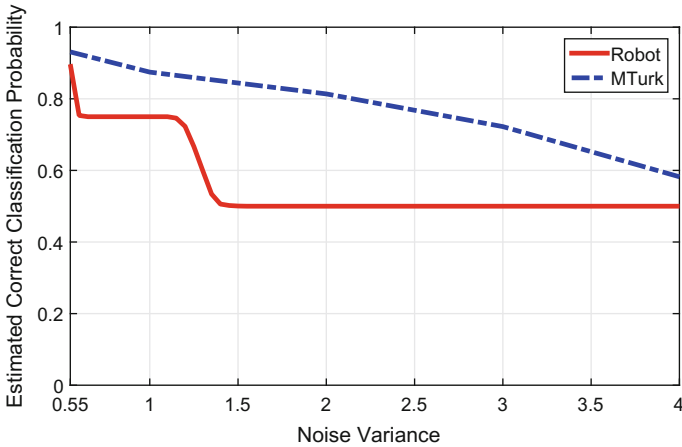


Fig. 12.2 Human and robot performance curves in target classification when additive noise is the main source of performance degradation [4]. The human data is acquired using Amazon MTurk. For more details, see [4] (© 2015 IEEE. Reprinted, with permission, from [4])

While this is a toy example, it captures a possible realistic scenario if additive noise is the main source of performance degradation. For instance, the robot may be able to assess its noise variance based on its distance to the target in the field but may not know the mean of the added noise or the nonlinear truncation that has happened at the pixel level. Our proposed approach of the next section will then utilize these performance curves for the optimization of the overall performance. We refer the readers to [5] for a more comprehensive prediction of human visual performance for any input with any source of uncertainty.

12.3 Optimizing Human–Robot Collaboration for Target Classification

We consider a setup in which the robots have an initial assessment (in the form of acquired images) of N given sites. Each robot is given an individual motion energy budget and they share a limited number of questions to ask the human operator. Two multi-robot scenarios are considered in this section. In the first scenario, it is assumed that each robot is assigned to a predetermined set of sites to classify. For each site that belongs to a robot’s assigned set, the robot has three choices: (1) rely on its own classification (based on the initial sensing), (2) use a question and present the data of the site to the human, or (3) spend motion energy to go to the site and sense it better. The robot’s second decision of asking the human for help is affected by the other robots’ decisions since they share a common number of allowed queries to the remote operator. By studying this case, we capture a realistic situation in which the robots explore the environment and perform their own tasks in geographically separated locations while being monitored by the same remote human operator. In the second scenario, we incorporate site allocation into the optimization framework. Based on the initial sensing, each robot’s motion energy cost to visit the sites, and the total number of allowed questions, the collaboration framework determines the sites the robots should query the human about, the sites for which they should rely on the initial sensing and the sites that should be visited. If a site is to be visited, the collaboration approach also determines which robot should visit that site.

12.3.1 Predetermined Site Allocation

In this section, we first discuss the case with a predetermined site allocation. Consider the case where we have a total number of K robots and each robot is assigned a priori to a set of N_k sites. There is a total of $N = \sum_{k=1}^K N_k$ sites. The sensing model of the robots is the same as explained in the previous section. In summary, each site contains one of T a priori known targets (see Fig. 12.1 (left) for an example with $T = 4$ targets). The sensing is then corrupted by an additive Gaussian noise with an unknown mean but a known variance, and is then truncated. The probabilities of correct target classification of the i th site assigned to robot k , for $k \in \{1, \dots, K\}$ and $i \in \{1, \dots, N_k\}$, are denoted by $p_{r,k,i}$ and $p_{h,k,i}$ for the robot and the human, respectively. These probabilities are obtained from Fig. 12.2, based on the variance assessed during the initial sensing. Note that although we assume a specific form of sensing uncertainty (additive Gaussian noise) here, our proposed optimization framework is general in that it only requires estimates of the human’s and the robot’s correct classification probabilities given a sensing input. The robots share a total of M allowed questions to the remote human operator and each robot has an individual motion energy budget of $\mathcal{E}_{max,k}$, where k is the index of the robot. Let $\mathcal{E}_{k,i}$ denote the motion energy cost to visit the i th site for the k th robot, which can be numerically

evaluated by the robot. If a robot chooses to visit a site, the probability of correct classification increases to a high value of $\tilde{p} \geq p_{r,k,i}, \forall k = 1, \dots, K, i = 1, \dots, N_k$. The objective of this collaboration is then to decide which sites to present to the human, which sites to visit and which sites to rely on the robots' own classification based on the initial sensing, in order to maximize the overall average probability of correct classification under resource constraints. Let p_c denote the average probability of correct classification of a site. We have

$$\begin{aligned} p_c &= \frac{1}{N} \sum_{k=1}^K \left(\sum_{i=1}^{N_k} \gamma_{k,i} p_{h,k,i} + \sum_{i=1}^{N_k} \eta_{k,i} \tilde{p} + \sum_{i=1}^{N_k} (1 - \gamma_{k,i})(1 - \eta_{k,i}) p_{r,k,i} \right), \\ &= \frac{1}{N} \sum_{k=1}^K \left(\sum_{i=1}^{N_k} \gamma_{k,i} (p_{h,k,i} - p_{r,k,i}) + \sum_{i=1}^{N_k} \eta_{k,i} (\tilde{p} - p_{r,k,i}) + \sum_{i=1}^{N_k} p_{r,k,i} \right), \end{aligned}$$

where $\gamma_{k,i}$ is 1 if robot k seeks human's help for its i th site and is 0 otherwise. Similarly, $\eta_{k,i} = 1$ indicates that robot k will visit its i th site and $\eta_{k,i} = 0$ denotes otherwise. We then have the following optimization problem:

$$\begin{aligned} \max_{\gamma, \eta} \quad & \sum_{k=1}^K \gamma_k^T (p_{h,k} - p_{r,k}) + \eta_k^T (\tilde{p} \mathbf{1} - p_{r,k}) \\ \text{s.t.} \quad & \eta_k^T \mathcal{E}_k \leq \mathcal{E}_{\max,k}, \quad \forall k = 1, \dots, K, \\ & \sum_{k=1}^K \gamma_k^T \mathbf{1} \leq M, \\ & \gamma_k + \eta_k \leq \mathbf{1}, \quad \forall k = 1, \dots, K, \\ & \gamma, \eta \in \{0, 1\}^N, \end{aligned} \tag{12.1}$$

where K is the total number of robots, N_k is the total number of sites that robot k needs to classify, $\mathcal{E}_{\max,k}$ is the motion energy budget for robot k , M is the number of allowed questions for all the robots, $p_{h,k} = [p_{h,k,1}, \dots, p_{h,k,N_k}]^T$, $p_{r,k} = [p_{r,k,1}, \dots, p_{r,k,N_k}]^T$, $\gamma_k = [\gamma_{k,1}, \dots, \gamma_{k,N_k}]^T$, $\eta_k = [\eta_{k,1}, \dots, \eta_{k,N_k}]^T$, $\mathcal{E}_k = [\mathcal{E}_{k,1}, \dots, \mathcal{E}_{k,N_k}]^T$, $\gamma = [\gamma_1^T, \dots, \gamma_K^T]^T$, $\eta = [\eta_1^T, \dots, \eta_K^T]^T$ and $N = \sum_{k=1}^K N_k$. The second constraint shows the coupling among the robots since they are all querying the same human operator, without which the optimization would be separable.

It can be seen that $(p_{h,k} - p_{r,k})$ and $(\tilde{p} \mathbf{1} - p_{r,k})$ are important parameters as they represent the performance gains by asking the human and visiting the sites, respectively. Note that we do not allow the robots to both query the human and make a visit for the same site. This is because we have already assumed a high probability of correct classification when a robot visits a site. Thus, allowing the robots to both visit and ask about the same site will be a waste of resources in this case.

12.3.1.1 Zero Motion Energy

If $\mathcal{E}_{max,k} = 0, \forall k = 1, \dots, K$, problem (12.1) reduces to a 0–1 Knapsack Problem [11], which is a combinatorial optimization problem that often arises in resource allocation scenarios. In this case, the robots only need to decide between asking the human and relying on the initial classification, which is shown below.

$$\begin{aligned} \max_{\bar{\gamma}} \quad & \bar{\gamma}^T (\bar{p}_h - \bar{p}_r) \\ \text{s.t.} \quad & \bar{\gamma}^T \mathbf{1} \leq M, \\ & \bar{\gamma} \in \{0, 1\}^N, \end{aligned} \quad (12.2)$$

where $\bar{p}_h = [\bar{p}_{h,1}, \dots, \bar{p}_{h,N}]$, $\bar{p}_r = [\bar{p}_{r,1}, \dots, \bar{p}_{r,N}]$, $\bar{p}_{h,i}$ and $\bar{p}_{r,i}$ denote the human's and the robot's correct classification probabilities of a site $i \in \{1, \dots, N\}$, $\bar{\gamma} = [\bar{\gamma}_1, \dots, \bar{\gamma}_N]$ and $\bar{\gamma}_i$ indicates whether the robots seek human help for site i . The optimal solution to this simplified problem can be obtained easily, which is summarized in the following lemma.

Lemma 12.1 *Suppose that all the N sites are sorted in a descending order according to $\bar{p}_{h,i} - \bar{p}_{r,i}$ such that $\bar{p}_{h,i} - \bar{p}_{r,i} \geq \bar{p}_{h,j} - \bar{p}_{r,j}$ for $i \leq j$. The optimal solution to problem (12.2) is given by*

$$\begin{aligned} \bar{\gamma}_i &= 1, \quad \text{for } i = 1, \dots, n, \\ \bar{\gamma}_i &= 0, \quad \text{for } i = n + 1, \dots, N, \end{aligned} \quad (12.3)$$

where $\sum_{i=1}^n \bar{\gamma}_i = M$.

Proof The results can be easily verified. □

12.3.1.2 Zero Number of Allowed Queries

If $M = 0$, problem (12.1) reduces to K separable 0–1 Knapsack Problems. The optimization problem for the k th robot is shown as follows.

$$\begin{aligned} \max_{\eta_k} \quad & \eta_k^T (\tilde{p} \mathbf{1} - p_{r,k}) \\ \text{s.t.} \quad & \eta_k^T \mathcal{E}_k \leq \mathcal{E}_{max,k}, \\ & \eta_k \in \{0, 1\}^{N_k}. \end{aligned} \quad (12.4)$$

Although the optimal solution to optimization problem (12.4) cannot be written directly in this case, its Linear Program (LP) relaxation provides a very close approximation. The LP relaxation of problem (12.4) is obtained by replacing the last binary constraint with $\eta_k \in [0, 1]^{N_k}$.

Lemma 12.2 *Suppose that the sites are sorted in a descending order according to $(\tilde{p} - p_{r,k,i})/\mathcal{E}_{k,i}$ such that $(\tilde{p} - p_{r,k,i})/\mathcal{E}_{k,i} \geq (\tilde{p} - p_{r,k,j})/\mathcal{E}_{k,j}$ for $i \leq j$. The optimal solution to the LP relaxation of problem (12.4) is given by*

$$\begin{aligned} \eta_{k,i} &= 1, \quad \text{for } i = 1, \dots, n-1, \\ \eta_{k,i} &= 0, \quad \text{for } i = n+1, \dots, N_k, \\ \eta_{k,n} &= \frac{\bar{\mathcal{E}}}{\mathcal{E}_n}, \end{aligned}$$

where $\bar{\mathcal{E}} = \mathcal{E}_{\max,k} - \sum_{i=1}^{n-1} \mathcal{E}_{k,i}$ and $n = \min\{j : \sum_{i=1}^j \mathcal{E}_{k,i} > \mathcal{E}_{\max,k}\}$.

Proof A graphical proof can be found in [9] and a more formal proof can be found in [11]. \square

12.3.1.3 Considering the General Case

Problem (12.1) is in general a Mixed Integer Linear Program (MILP), which makes theoretical analysis difficult. In order to bring a more analytical understanding to this problem, we consider the following LP relaxation of problem (12.1), which is a close approximation to the problem. The LP relaxation allows the decision variables γ and η to take continuous values between 0 and 1.

$$\begin{aligned} \max_{\gamma, \eta} \quad & \sum_{k=1}^K \gamma_k^T (p_{h,k} - p_{r,k}) + \eta_k^T (\tilde{p}\mathbf{1} - p_{r,k}) \\ \text{s.t.} \quad & \eta_k^T \mathcal{E}_k \leq \mathcal{E}_{\max,k}, \quad \forall k = 1, \dots, K, \\ & \sum_{k=1}^K \gamma_k^T \mathbf{1} \leq M, \\ & \gamma_k + \eta_k \leq \mathbf{1}, \quad \forall k = 1, \dots, K, \\ & \gamma, \eta \in [0, 1]^N. \end{aligned} \tag{12.5}$$

We can analyze this LP by applying Karush–Kuhn–Tucker (KKT) conditions [1]. We then have the following expression for the Lagrangian:

$$\begin{aligned} \mathcal{L}(\gamma, \eta, \omega, \lambda_1, \lambda_2, \theta, \zeta, \kappa, \tau, \xi, \psi) &= - \left(\sum_{k=1}^K \gamma_k^T (p_{h,k} - p_{r,k}) + \eta_k^T (\tilde{p}\mathbf{1} - p_{r,k}) \right) \\ &+ \mu \left(\sum_{k=1}^K \mathbf{1}^T \gamma_k - M \right) + \sum_{k=1}^K \lambda_k (\eta_k^T \mathcal{E}_k - \mathcal{E}_{\max,k}) + \theta^T (\gamma + \eta - \mathbf{1}) + \psi^T (\gamma - \mathbf{1}) \\ &- \phi^T \gamma + \kappa^T (\eta - \mathbf{1}) - \omega^T \eta, \end{aligned}$$

where $\mu, \lambda, \theta, \psi, \phi, \kappa, \omega$ are nonnegative Lagrange multipliers, and $\lambda = [\lambda_1, \dots, \lambda_K]$.

The optimal solution (marked by \star) then satisfies the following KKT conditions, in addition to the primal/dual feasibility conditions:

(1) Gradient condition, for $k \in \{1, \dots, K\}$ and $i \in \{1, \dots, N_k\}$:

$$\nabla_{\gamma_{k,i}^*} \mathcal{L} = p_{r,k,i} - p_{h,k,i} + \mu^* + \theta_{k,i}^* + \psi_{k,i}^* - \phi_{k,i}^* = 0, \quad (12.6)$$

$$\nabla_{\eta_{k,i}^*} \mathcal{L} = p_{r,k,i} - \tilde{p} + \lambda_k^* \mathcal{E}_{k,i} + \theta_{k,i}^* + \kappa_{k,i}^* - \omega_{k,i}^* = 0. \quad (12.7)$$

(2) Complementary slackness: $\theta^* \circ (\gamma^* + \eta^* - 1) = \mathbf{0}$, $\psi^* \circ (\gamma^* - 1) = \mathbf{0}$, $\phi^* \circ \gamma^* = \mathbf{0}$, $\kappa^* \circ (\eta^* - 1) = \mathbf{0}$, $\omega^* \circ \eta^* = \mathbf{0}$, $\mu^* (\sum_{k=1}^K \mathbf{1}^T \gamma_k - M) = 0$, $\lambda \circ (\eta^T \mathcal{E} - \mathcal{E}_{max}) = \mathbf{0}$, where $\mathbf{0}$ denotes the vector with all entries equal to 0, \circ denotes the Hadamard product, $\mathcal{E} = [\mathcal{E}_1^T, \dots, \mathcal{E}_K^T]^T$ and $\mathcal{E}_{max} = [\mathcal{E}_{max,1}, \dots, \mathcal{E}_{max,k}]^T$.

The following lemmas characterize the optimal solution to the LP relaxation in terms of the optimization parameters.

Lemma 12.3 Consider two sites i and j that belong to the preassigned sets of robot k_1 and robot k_2 , respectively.¹ Let γ^* and η^* denote the optimal decision vectors. If $\gamma_{k_1,i}^* = 1$, $\eta_{k_1,i}^* = 0$, $\gamma_{k_2,j}^* = 0$ and $\eta_{k_2,j}^* = 0$, then $p_{h,k_1,i} - p_{r,k_1,i} \geq p_{h,k_2,j} - p_{r,k_2,j}$.

Proof Suppose that we have two sites i and j preassigned to robot k_1 and robot k_2 respectively such that $\gamma_{k_1,i}^* = 1$, $\eta_{k_1,i}^* = 0$, $\gamma_{k_2,j}^* = 0$ and $\eta_{k_2,j}^* = 0$. Applying the complementary slackness conditions results in $\phi_{k_1,i}^* = \theta_{k_2,j}^* = \phi_{k_2,j}^* = 0$. Then the gradient condition gives $p_{r,k_1,i} - p_{h,k_1,i} + \theta_{k_1,i}^* + \phi_{k_1,i}^* = p_{r,k_2,j} - p_{h,k_2,j} - \phi_{k_2,j}^*$. Since $\theta_{k_1,i}^*$, $\phi_{k_1,i}^*$ and $\psi_{k_2,j}^*$ are all nonnegative, it is necessary to have $p_{h,k_1,i} - p_{r,k_1,i} \geq p_{h,k_2,j} - p_{r,k_2,j}$. \square

Lemma 12.3 says that if we have any two sites i and j , for which the robots will ask the human and rely on the initial sensing respectively, then the performance gain obtained from querying the human operator for site i should be higher than or equal to that of site j .

Remark 12.1 Lemma 12.3 also holds for the original integer problem (12.1).

Lemma 12.4 Consider two sites i and j that have been assigned to robot k . Let γ^* and η^* denote the optimal decision vectors. If $\gamma_{k,i}^* = 0$, $\eta_{k,i}^* = 1$, $\gamma_{k,j}^* = 0$ and $\eta_{k,j}^* = 0$, then $(\tilde{p} - p_{r,k,i})/\mathcal{E}_{k,i} \geq (\tilde{p} - p_{r,k,j})/\mathcal{E}_{k,j}$.

Proof Suppose that we have two sites i and j assigned to robot k such that $\gamma_{k,i}^* = 0$, $\eta_{k,i}^* = 1$, $\gamma_{k,j}^* = 0$ and $\eta_{k,j}^* = 0$. We have $\omega_{k,i}^* = \theta_{k,j}^* = \kappa_{k,j}^* = 0$ from the complementary slackness conditions. Equation 12.7 for $\eta_{k,i}^*$ then becomes: $(p_{r,k,i} - \tilde{p})/\mathcal{E}_{k,i} + \lambda_k^* + \theta_{k,i}^* + \kappa_{k,i}^* = 0$, where $\theta_{k,i}^* = \theta_{k,i}^*/\mathcal{E}_{k,i}$ and $\kappa_{k,i}^* = \kappa_{k,i}^*/\mathcal{E}_{k,i}$. Similarly, we have $(p_{r,k,j} - \tilde{p})/\mathcal{E}_{k,j} + \lambda_k^* - \omega_{k,j}^* = 0$ when applying $\nabla_{\eta_{k,j}^*} \mathcal{L} = 0$. This results in $(p_{r,k,i} - \tilde{p})/\mathcal{E}_{k,i} + \lambda_k^* + \theta_{k,i}^* + \kappa_{k,i}^* = (p_{r,k,j} - \tilde{p})/\mathcal{E}_{k,j} + \lambda_k^* - \omega_{k,j}^*$. Since $\theta_{k,i}^*$, $\kappa_{k,i}^*$ and $\omega_{k,j}^*$ are all nonnegative, we have $(\tilde{p} - p_{r,k,i})/\mathcal{E}_{k,i} \geq (\tilde{p} - p_{r,k,j})/\mathcal{E}_{k,j}$. \square

¹Note that robot k_1 and robot k_2 can be the same robot or two different robots.

Lemma 12.4 says that within the set of sites assigned to a robot, if there are two sites i and j , for which the robot will explore and rely on the initial sensing respectively, then the visited site should have a higher performance gain normalized by the energy cost.²

Lemma 12.5 *Consider two sites i and j that have been assigned to robot k . Let γ^* and η^* denote the optimal decision vectors. If $\gamma_{k,i}^* = 1, \eta_{k,i}^* = 0, \gamma_{k,j}^* = 0, \eta_{k,j}^* = 1$ and $\mathcal{E}_{k,i} \leq \mathcal{E}_{k,j}$, then $p_{h,k,i} - p_{h,k,j} \geq 0$.*

Proof Consider an optimal solution where we have $\gamma_{k,i}^* = 1, \eta_{k,i}^* = 0, \gamma_{k,j}^* = 0, \eta_{k,j}^* = 1$ and $\mathcal{E}_{k,i} \leq \mathcal{E}_{k,j}$. We modify the current optimal solution to obtain a new feasible solution in the following way: $\gamma'_{k,i} = \gamma_{k,i}^* - \delta, \eta'_{k,i} = \eta_{k,i}^* + \delta, \gamma'_{k,j} = \gamma_{k,j}^* + \delta, \eta'_{k,j} = \eta_{k,j}^* - \delta$, where $\delta > 0$ is a small number such that $\gamma'_{k,i}, \eta'_{k,i}, \gamma'_{k,j}, \eta'_{k,j} \in [0, 1]$. The new objective function value becomes $f' = f^* + \Delta$, where f^* is the optimum and $\Delta = \delta(\tilde{p} - p_{r,k,i} - (p_{h,k,i} - p_{r,k,i}) + p_{h,k,j} - p_{r,k,j} - (\tilde{p} - p_{r,k,j}))$. Since the current solution is optimal, we should have $\Delta \leq 0$, from which we have $p_{h,k,i} - p_{h,k,j} \geq 0$. \square

Consider the case where sites i and j are assigned to robot k . The robot asks for human help for site i and visits site j in the optimal solution. Lemma 12.5 says that in this case, if the motion energy cost of the queried site is less than or equal to that of the visited site, then the human performance of the queried site should be greater than or equal to that of the visited site.

12.3.2 Optimized Site Allocation

In this section, we consider the second collaborative scenario with a human operator and multiple field robots described earlier, where the optimization of site allocation to the robots is also taken into account. Consider the case where there is a total of N sites and K robots. The sensing model is the same as discussed in the previous section. The probabilities of correct target classification of the i th site are denoted by $\tilde{p}_{r,i}$ and $\tilde{p}_{h,i}$ for the robot and the human, respectively. These probabilities are obtained from Fig. 12.2, based on the variance assessed during the initial sensing. The robots share a total of M allowed questions to the remote human operator and each robot has an individual motion energy budget of $\mathcal{E}_{max,k}$, where k is the index of the robot. Let $\tilde{\mathcal{E}}_{k,i}$ denote the motion energy cost to visit the i th site for the k th robot. If a robot chooses to visit a site, the probability of correct classification increases to a high value of \tilde{p} . The objective of this collaboration is for the robots to decide on which sites to present to the human, which sites to rely on the initial sensing and which sites to visit. If a site is to be visited, this collaboration also determines which robot should visit the site. Let \tilde{p}_c denote the average probability of correct classification of a site, which we would like to maximize. We have

²This lemma is similar to the second condition of Lemma 12.1 of our previous work [4] as it concerns only one robot.

$$\begin{aligned}\tilde{p}_c &= \frac{1}{N} \left(\sum_{k=1}^K \sum_{i=1}^N \tilde{\eta}_{k,i} \tilde{p} + \sum_{i=1}^N \tilde{\gamma}_i \tilde{p}_{h,i} + \sum_{i=1}^N (1 - \tilde{\gamma}_i) \left(1 - \sum_{k=1}^K \tilde{\eta}_{k,i} \right) \tilde{p}_{r,i} \right), \\ &= \frac{1}{N} \left(\sum_{i=1}^N \tilde{\gamma}_i (\tilde{p}_{h,i} - \tilde{p}_{r,i}) + \sum_{k=1}^K \sum_{i=1}^N \tilde{\eta}_{k,i} (\tilde{p} - \tilde{p}_{r,i}) + \sum_{i=1}^N \tilde{p}_{r,i} \right),\end{aligned}$$

where $\tilde{\gamma}_i$ is 1 if the robots seek human's help for the i th site and is 0 otherwise. Similarly, $\tilde{\eta}_{k,i} = 1$ indicates that robot k will visit the i th site and $\tilde{\eta}_{k,i} = 0$ denotes otherwise. The optimization problem is then given by

$$\begin{aligned}\max_{\tilde{\gamma}, \tilde{\eta}} \quad & \sum_{k=1}^K \tilde{\eta}_k^T (\tilde{p} \mathbf{1} - \tilde{p}_r) + \tilde{\gamma}^T (\tilde{p}_h - \tilde{p}_r) \\ \text{s.t.} \quad & \tilde{\eta}_k^T \tilde{\mathcal{E}}_k \leq \mathcal{E}_{\max,k}, \quad \forall k = 1, \dots, K, \\ & \tilde{\gamma}^T \mathbf{1} \leq M, \\ & \tilde{\gamma} + \sum_{k=1}^K \tilde{\eta}_k \leq \mathbf{1}, \\ & \tilde{\gamma}, \tilde{\eta}_k \in \{0, 1\}^N, \quad \forall k = 1, \dots, K,\end{aligned}\tag{12.8}$$

where K is the total number of robots, N is the total number of sites to classify, $\mathcal{E}_{\max,k}$ is the motion energy budget for robot k , M is the total number of allowed questions, $\tilde{p}_h = [\tilde{p}_{h,1}, \dots, \tilde{p}_{h,N}]^T$, $\tilde{p}_r = [\tilde{p}_{r,1}, \dots, \tilde{p}_{r,N}]^T$, $\tilde{\gamma} = [\tilde{\gamma}_1, \dots, \tilde{\gamma}_N]^T$, $\tilde{\eta}_k = [\tilde{\eta}_{k,1}, \dots, \tilde{\eta}_{k,N}]^T$, $\tilde{\eta} = [\tilde{\eta}_1^T, \dots, \tilde{\eta}_K^T]^T$ and $\tilde{\mathcal{E}}_k = [\tilde{\mathcal{E}}_{k,1}, \dots, \tilde{\mathcal{E}}_{k,N}]^T$. $\tilde{\gamma}$ and $\tilde{\eta}$ determine whether the robots should ask for human help and visit the sites, respectively.

Problem (12.8) is in the form of a Multiple Knapsack Problems (MKP) [11], which is a natural extension to the basic 0–1 Knapsack Problem discussed in the previous section. This problem arises commonly in optimal decision-making and resource allocation settings.

12.3.2.1 Zero Motion Energy

If $\mathcal{E}_{\max,k} = 0$, $\forall k = 1, \dots, K$, problem (12.8) reduces to a 0–1 Knapsack Problem.

$$\begin{aligned}\max_{\tilde{\gamma}} \quad & \tilde{\gamma}^T (\tilde{p}_h - \tilde{p}_r) \\ \text{s.t.} \quad & \tilde{\gamma}^T \mathbf{1} \leq M, \\ & \tilde{\gamma} \in \{0, 1\}^N.\end{aligned}\tag{12.9}$$

The above-reduced problem is very similar to problem (12.2) discussed previously. The optimal solution to this special case can be obtained via the same procedure outlined in Lemma 12.1.

12.3.2.2 Considering the General Case

In order to bring a more theoretical understanding to this setting, we consider the LP relaxation of problem (12.8), which is given as follows.

$$\begin{aligned}
& \max_{\tilde{\gamma}, \tilde{\eta}} \sum_{k=1}^K \tilde{\eta}_k^T (\tilde{p}\mathbf{1} - \tilde{p}_r) + \tilde{\gamma}^T (\tilde{p}_h - \tilde{p}_r) \\
& \text{s.t. } \tilde{\eta}_k^T \tilde{\mathcal{E}}_k \leq \mathcal{E}_{\max,k}, \quad \forall k = 1, \dots, K, \\
& \quad \tilde{\gamma}^T \mathbf{1} \leq M, \\
& \quad \tilde{\gamma} + \sum_{k=1}^K \tilde{\eta}_k \leq \mathbf{1}, \\
& \quad \tilde{\gamma}, \tilde{\eta}_k \in [0, 1]^N, \quad \forall k = 1, \dots, K.
\end{aligned} \tag{12.10}$$

By allowing the decision variables $\tilde{\gamma}$ and $\tilde{\eta}$ to take continuous values in the interval $[0, 1]$, we can analyze this problem utilizing the KKT conditions, which leads to the following two lemmas.

Lemma 12.6 *Consider two sites i and j . Let $\tilde{\gamma}^*$ and $\tilde{\eta}^*$ denote the optimal decision vectors. If $\tilde{\gamma}_i^* = 1$, $\sum_{k=1}^K \tilde{\eta}_{k,i}^* = 0$, $\tilde{\gamma}_j^* = 0$ and $\sum_{k=1}^K \tilde{\eta}_{k,j}^* = 0$, then $\tilde{p}_{h,i} - \tilde{p}_{r,i} \geq \tilde{p}_{h,j} - \tilde{p}_{r,j}$.*

Proof The proof is similar to that of Lemma 12.3. □

Lemma 12.6 says that if we have two sites i and j , for which the robots will ask the human and rely on the initial sensing respectively, then the performance gain obtained from asking the human should be greater for site i .

Remark 12.2 Lemma 12.6 also holds for the original integer problem (12.8).

Lemma 12.7 *Consider two sites i and j . Let $\tilde{\gamma}^*$ and $\tilde{\eta}^*$ denote the optimal decision vectors. If $\tilde{\gamma}_i^* = 0$, $\tilde{\eta}_{k_1,i}^* = 1$, $\tilde{\gamma}_j^* = 0$ and $\sum_{k=1}^K \tilde{\eta}_{k,j}^* = 0$, then $(\tilde{p} - \tilde{p}_{r,i})/\tilde{\mathcal{E}}_{k_1,i}^* \geq (\tilde{p} - \tilde{p}_{r,j})/\tilde{\mathcal{E}}_{k_1,j}^*$, where k_1 is the index of the robot that visits site i .*

Proof The proof is similar to that of Lemma 12.4. □

Consider two sites i and j . Suppose that in an optimal solution, site i is visited by robot k_1 and the classification of site j is based on the initial sensing. Lemma 12.7 says that the performance gain obtained from further sensing normalized by robot k_1 's motion energy cost should be higher for site i as compared to site j .

Lemma 12.8 *Consider two sites i and j . Let $\tilde{\gamma}^*$ and $\tilde{\eta}^*$ denote the optimal decision vectors. If $\tilde{\gamma}_i^* = 1$, $\tilde{\eta}_{k,j}^* = 1$ and $\tilde{\mathcal{E}}_{k,i}^* \leq \tilde{\mathcal{E}}_{k,j}^*$, then $\tilde{p}_{h,i} - \tilde{p}_{h,j} \geq 0$.*

Proof The proof is similar to that of Lemma 12.5. □

Consider two sites i and j . Suppose that in an optimal solution, the robots query the human about site i and have robot k visit site j . Lemma 12.8 says that in this case, if robot k 's motion energy cost of the queried site is less than or equal to that of the visited site, then the human performance of the queried site should be greater than or equal to that of the visited site.

Lemma 12.9 *Consider two sites i and j and two robots k_1 and k_2 . Let $\tilde{\gamma}^*$ and $\tilde{\eta}^*$ denote the optimal motion decision vectors. Suppose that $\tilde{\eta}_{k_1,i}^* = 1$, $\tilde{\eta}_{k_2,j}^* = 1$ and $\exists m \in \{1, \dots, N\}$ such that $\tilde{\gamma}_m^* = 0$ and $\sum_{k=1}^K \tilde{\eta}_{k,m}^* = 0$. Then the following conditions must hold.*

- (1) $\tilde{\mathcal{E}}_{k_1,i} \leq \tilde{\mathcal{E}}_{k_1,j}$ or $\tilde{\mathcal{E}}_{k_2,i} \geq \tilde{\mathcal{E}}_{k_2,j}$;
- (2) If $\tilde{\mathcal{E}}_{k_1,i} \leq \tilde{\mathcal{E}}_{k_1,j}$, then $\tilde{\mathcal{E}}_{k_2,j} - \tilde{\mathcal{E}}_{k_2,i} \leq \tilde{\mathcal{E}}_{k_1,j} - \tilde{\mathcal{E}}_{k_1,i}$;
- (3) If $\tilde{\mathcal{E}}_{k_2,i} \geq \tilde{\mathcal{E}}_{k_2,j}$, then $\tilde{\mathcal{E}}_{k_1,i} - \tilde{\mathcal{E}}_{k_1,j} \leq \tilde{\mathcal{E}}_{k_2,i} - \tilde{\mathcal{E}}_{k_2,j}$.

Proof (1) Suppose that $\tilde{\mathcal{E}}_{k_1,i} \geq \tilde{\mathcal{E}}_{k_1,j}$ and $\tilde{\mathcal{E}}_{k_2,i} \leq \tilde{\mathcal{E}}_{k_2,j}$. We can let $\tilde{\eta}'_{k_1,i} = 0$, $\tilde{\eta}'_{k_1,j} = 1$, $\tilde{\eta}'_{k_2,i} = 1$ and $\tilde{\eta}'_{k_2,j} = 0$, which will give us the same objective function value but with a less motion energy consumption. The residual energy can be utilized such that $\tilde{\eta}'_{k_1,m} = \delta_{k_1}$ and $\tilde{\eta}'_{k_2,m} = \delta_{k_2}$, where δ_{k_1} and δ_{k_2} are small positive numbers. This constructed solution will be strictly better than the current optimal solution, which is a contradiction. Thus we must have $\tilde{\mathcal{E}}_{k_1,i} \leq \tilde{\mathcal{E}}_{k_1,j}$ or $\tilde{\mathcal{E}}_{k_2,i} \geq \tilde{\mathcal{E}}_{k_2,j}$.

(2) and (3) If Condition (2) or (3) fails, we can construct a new feasible solution in a similar way as in the proof of Condition (1), which will be strictly better than the current optimal solution, resulting in a contradiction. \square

Consider the case where there exists at least one site, for which the robots will rely on the initial sensing. The first part of Lemma 12.9 says that in this case, if two sites i and j are visited by two robots k_1 and k_2 respectively, then either it should be less costly for robot k_1 to visit site i as compared to site j or it should be less costly for robot k_2 to visit site j as compared to site i . Furthermore, the second part of the lemma says that if it is less costly for robot k_1 to visit site i as compared to site j ($\tilde{\mathcal{E}}_{k_1,i} \leq \tilde{\mathcal{E}}_{k_1,j}$), then robot k_2 's motion energy cost of visiting site j should not exceed that of site i by $\tilde{\mathcal{E}}_{k_1,j} - \tilde{\mathcal{E}}_{k_1,i}$, which can be thought of as the motion energy saving of robot k_1 . The third part can be interpreted in a similar manner. This lemma basically shows that the robots' decisions should be efficient in terms of motion energy usage.

12.4 Numerical Results

In this section, we show the performance of our collaboration design for field exploration and target classification. We first summarize the results for a case where there is only one robot [4] to gain a more intuitive understanding of the optimal behavior that arises from our optimization framework. We then show the numerical results for the case of multiple robots. The optimization problems are solved with the MILP solver of MATLAB by using the collected MTurk data of Fig. 12.2.

12.4.1 Collaboration Between the Human Operator and One Robot [4]

Consider the case where there is only one robot in the field. In this case, both multi-robot formulations (problems (12.1) and (12.8)) reduce to the same optimization problem, which is shown as follows.

$$\begin{aligned}
 \max_{\gamma, \eta} \quad & \gamma^T (p_h - p_r) + \eta^T (\tilde{p}\mathbf{1} - p_r) \\
 \text{s.t.} \quad & \eta^T \mathcal{E} \leq \mathcal{E}_{\max}, \quad \mathbf{1}^T \gamma \leq M, \\
 & \gamma + \eta \leq \mathbf{1}, \\
 & \gamma, \eta \in \{0, 1\}^N.
 \end{aligned} \tag{12.11}$$

In order to better understand the optimal solution, Fig. 12.3 shows an example of the optimal decisions for the case of 2000 sites, with 500 allowed questions and an energy budget equal to 25% of the total energy needed to visit all the sites. The optimal decision for each site is marked based on solving problem (12.11). Interesting behavior emerges as can be seen. For instance, we can observe that there are clear separations between different decisions. The clearest patterns are two transition points that mark when the robot asks the human operator for help, as shown with

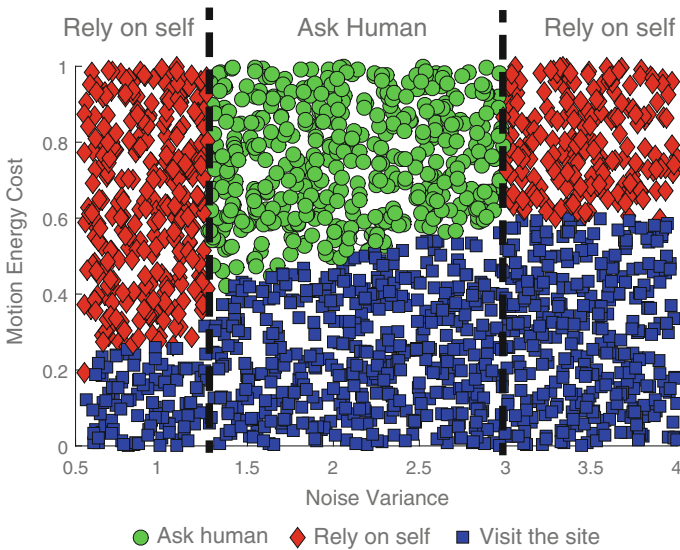


Fig. 12.3 An example of the optimal decisions with 2000 sites, 500 questions, and an energy budget of 25% of the total energy needed to visit all the sites. In this example, the collaboration is between one operator and one robot. This result is from our previous work [4] (© 2015 IEEE. Reprinted, with permission, from [4])

the dashed vertical lines in Fig. 12.3. Basically, the figure suggests that the robot should not bug the human if the variance is smaller than a threshold or bigger than another threshold, independent of the motion cost of a site. This makes sense as the robot itself will perform well for low variances and humans do not perform well for high variances, suggesting an optimal query range. Furthermore, it shows that the robot is more willing to spend motion energy if the sensing of a site has higher noise variance. However, the robot in general only visits the sites where the energy cost is not too high and relies more on itself for the sites with both high variance and high energy cost.

In the following part, we show the energy and bandwidth savings of our proposed approach as compared to a benchmark methodology where human collaboration is not fully optimized. In the benchmark approach, the robot optimizes its given energy budget to best explore the field based on site variances, i.e., it chooses the sites that maximize the sum of noise variances. It then randomly chooses from the remaining sites to ask the human operator, given the total number of questions. In other words, the robot optimizes its energy usage without any knowledge of the human's performance.

12.4.1.1 Energy Saving

Table 12.1 shows the amount of motion energy the robot saves for achieving a desired probability of correct classification by using our approach as compared to the benchmark. The first column shows the desired average probability of correct classification and the second column shows the percentage reduction of the needed energy by using our proposed approach as compared to the benchmark method. In this case, there is a total of $N = 10$ sites and $M = 4$ given queries. The noise variance of each site is randomly assigned from the interval $[0.55, 4]$. \bar{p} is set to 0.896, which is the best achievable robot performance based on Fig. 12.2. The motion energy cost to visit each site is also assigned randomly and the total given energy budget is taken to be a percentage of the total energy required to visit all the sites. It can be seen that the robot can reduce its energy consumption considerably by properly taking advantage of its collaboration. For instance, it can achieve an average probability of correct

Table 12.1 Energy saving as compared to the benchmark in the one-operator-one-robot case (© 2015 IEEE. Reprinted, with permission, from [4])

Desired ave. correct classification prob.	Energy saving (in %)
0.7	66.67 %
0.75	44.30 %
0.8	27.83 %
0.85	6.3 %
0.9	0.71 %
0.915	Inf

classification of 0.7 with 66.67% less energy consumption. The term “Inf” denotes the cases where the benchmark cannot simply achieve the given target probability of correct classification.

12.4.1.2 Bandwidth Saving

Next, we show explicitly how our proposed approach can also result in a considerable communication bandwidth saving by reducing the number of questions. More specifically, consider the cases with “large bandwidth” and “zero bandwidth”. In the first case, the robot has no communication limitation and can probe the human with as many questions as it wants to (10 in this case). In the latter, no access to a human operator is available and thus the robot has to rely on itself to classify the gathered data after it surveys the field. Figure 12.4 compares the performance of our proposed approach with these two cases. The robot is given an energy budget of 30% of the total energy needed to visit all the sites.

As expected, the case of “no bandwidth” performs considerably poorly as the robot could not seek human help in classification. On the other hand, the case of “large bandwidth” performs considerably well as the robot can ask for the human operator’s help as many times as it wants. This, however, comes at a cost of excessive communication and thus a high bandwidth usage.³ It can be seen that our proposed approach can achieve a performance very close to this upper bound with a much less bandwidth usage. For instance, we can see that by asking only 6 questions (40% bandwidth reduction), the robot can achieve an average probability of correct classification of 0.888, which is only 4.3% less than the case of large bandwidth (0.928 in this case).

Table 12.2 shows the amount of bandwidth the robot can save by using our approach, when trying to achieve a desired average probability of correct classification. The first column shows the desired average probability of correct classification while the second column shows the percentage reduction of the needed bandwidth by using our proposed approach as compared to the benchmark. In this case, the robot is given an energy budget of 30% of the total energy needed to visit all the sites. It can be seen that the robot can reduce its bandwidth consumption considerably. For instance, it can achieve an average probability of correct classification of 0.75 with 48.61% less bandwidth usage.

12.4.2 Predetermined Site Allocation

In this section, we numerically demonstrate the efficacy of our approach for the one-operator-multi-robot collaborative scenario when the allocation of the sites to the robots is predetermined. We first show an interesting pattern that characterizes

³Bandwidth usage is taken proportional to the number of questions.

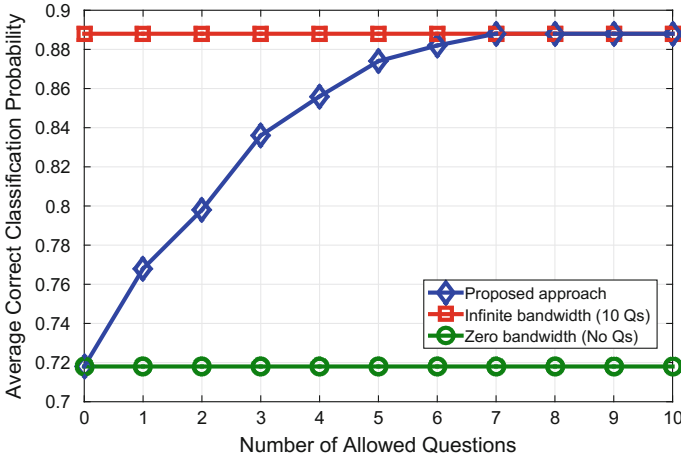


Fig. 12.4 Average probability of correct classification in the one-operator-one-robot collaboration as a function of the total number of given queries. In this example, there is a total of 10 sites and the given motion energy budget is 30% of what is needed to visit all the sites (© 2015 IEEE. Reprinted, with permission, from [4])

Table 12.2 Bandwidth saving as compared to the benchmark in a one-operator-one-robot case (© 2015 IEEE. Reprinted, with permission, from [4])

Desired ave. correct classification prob.	Bandwidth saving (in %)
0.7	37.04 %
0.75	48.61 %
0.8	33.18 %
0.85	7.33 %
0.875	Inf

the conditions under which the robots will visit the sites and ask for human’s help respectively. We then illustrate how our approach plans the collaborative operation by showing an example solution to problem (12.1), after which we conduct numerical evaluations to demonstrate how our proposed approach can save resources significantly.

12.4.2.1 Patterns of Optimal Decisions

We solve problem (12.1) with two robots, where each robot is assigned to 1000 sites. There is a total of 500 given queries and the energy budget is taken as 25% of what is needed to visit all the sites in the preassigned set for each robot. The noise variance of each site is randomly assigned from the interval [0.55, 4]. \tilde{p} is set to 0.896, which is the best achievable robot performance based on Fig. 12.2. The motion energy cost to visit each site is also assigned randomly.

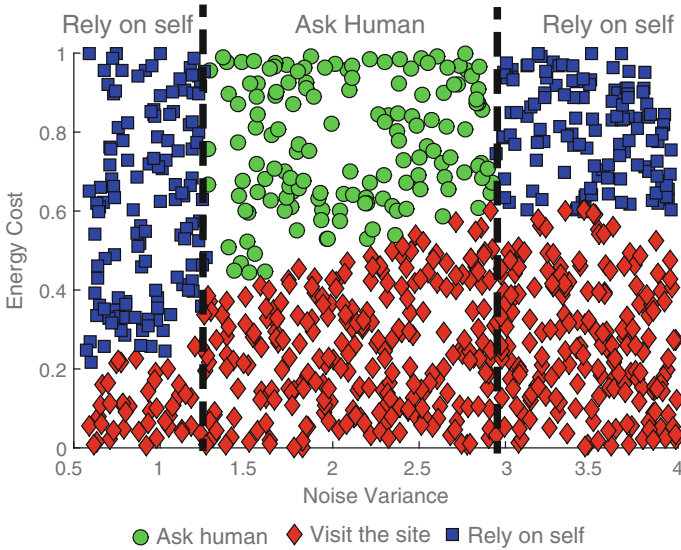


Fig. 12.5 An example of the optimal decisions with two robots. Each robot is assigned to 1000 sites and given an energy budget of 25% of the total energy needed to visit all its preassigned sites. The two robots share a total number of 500 questions. The figure shows the decisions of robot 1

Figure 12.5 shows the optimal decisions of the first robot with the above parameters. Green disks represent the decision of asking for human help, red diamonds represent the decision of visiting the site, and blue squares represent the decision of relying on the initial sensing. It can be seen that the optimal behavior of a robot in the one-operator-multi-robot setting is very similar to that of the one-operator-one-robot case. More specifically, the robot will only query the human operator about sites where the sites' sensing variance is not too low or too high. The robot is more willing to spend motion energy to move to sites with high noise variance for further sensing as long as the energy cost is not too high. The optimal decisions of the second robot have a similar pattern.

To better understand the impact of noise variance and motion energy cost on the optimal decisions, we conduct the following analysis. From Fig. 12.2, we can see that there is a noise variance range within which it is very beneficial to query the human operator ([1.5, 2.5]). Thus the distribution of the values of the noise variance will have a considerable impact on the optimal decisions. For instance, suppose that the noise variance of the sites is drawn from a Gaussian distribution that is mainly concentrated in the interval [1.5, 2.5]. Then, the robot can have a good gain from asking for help if its motion budget is not too large. To further understand these impacts, we perform simulations with two robots, each assigned to 200 sites. We vary the distribution of the noise variance and the given motion energy budgets for the two robots. Figure 12.6 shows the probability density functions (PDFs) of the two noise variance distributions that we will use in the simulations. The first (left)

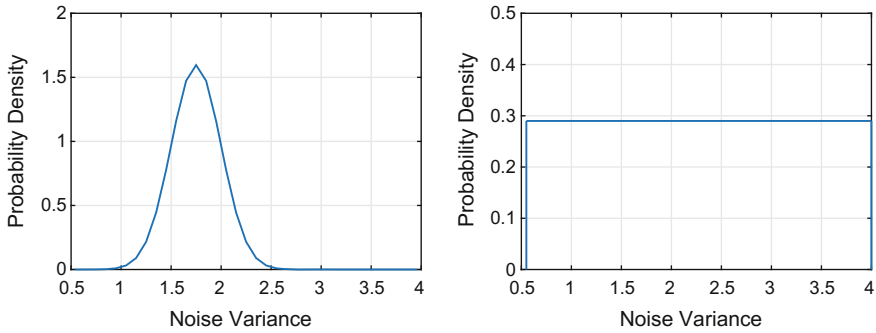


Fig. 12.6 (left) The PDF of the truncated Gaussian distribution. (right) The PDF of a uniform distribution. Both PDFs have the support of $[0.55, 4]$ and are used to generate noise variances in the simulations

is a truncated Gaussian distribution with mean 1.75 and variance 0.25. The values of the noise variance are truncated so that they stay inside the interval $[0.55, 4]$. The noise variance produced from this distribution will be mainly within the range where it is most beneficial to query the human operator based on Fig. 12.2. The second distribution is a uniform distribution over the interval $[0.55, 4]$.

Table 12.3 shows the average number of sites asked and visited by each robot. The noise variance of the sites of robot 1 is drawn from the uniform distribution while the noise variance of the sites of robot 2 is drawn from the truncated Gaussian distribution. There is a total of 100 allowed queries. Both robots are given 25% of what is needed to visit all sites from their respective sets. The motion energy cost to visit each site is assigned randomly. The results are averaged over multiple simulations so that the analysis is less dependent on the specific realizations of the two distributions. It can be seen that the average number of sites asked by robot 2 is significantly greater than that by robot 1. This is because the noise variance of the sites of robot 2 mainly lie within the range where it is more beneficial to ask for help. The average number of visited sites is almost the same for both robots as they are given the same energy budget in terms of the percentage of the total energy required to visit all the sites in their respective sets. Thus robot 1 has to rely more on the initial sensing for classification. As we increase the total number of allowed questions, we expect the difference between the number of questions used by the two robots to decrease.

Next, we fix the noise variance distribution and study how different motion energy budgets affect the optimal decisions. Table 12.4 shows the average number of sites asked and visited by each robot. The noise variance of the sites of both robots are drawn from the uniform distribution. There is a total of 100 allowed queries. In terms of energy budget, robot 1 and robot 2 are given 20 and 40% of what is needed to visit all the sites in their respective sets. It can be seen that the average number of queried sites by robot 1 is greater than that of robot 2. This makes sense since the number of visited sites by robot 1 is smaller due to the smaller energy budget.

Table 12.3 Average number of sites asked and visited by each robot. The noise variances for robot 1 and robot 2 are drawn from the uniform distribution and the truncated Gaussian distribution, respectively (see Fig. 12.6). Each robot is assigned to 200 sites and there is a total of 100 allowed queries. Each robot is given an energy budget of 25% of what is needed to visit all the sites in its respective set

	Ave. # of sites visited	Ave. # of sites asked
Robot 1	95.65	34.4
Robot 2	96.3	65.6

Table 12.4 Average number of sites asked and visited by each robot. The noise variances for both robots are drawn from the uniform distribution. Each robot is assigned to 200 sites and there is a total of 100 allowed queries. Robot 1 is given an energy budget of 20% of what is needed to visit all the sites in its set while robot 2 is given an energy budget of 40% of what is needed to visit all the sites in its set

	Ave. # of sites visited	Ave. # of sites asked
Robot 1	85.2	59.5
Robot 2	119.6	40.5

12.4.2.2 Example Solution

In this section, we study a sample solution to problem (12.1). We consider the case with two robots, each assigned to five sites. The noise variance of each site is randomly assigned from the interval $[0.55, 4]$. \bar{p} is set to 0.896. The motion energy cost to visit each site is assigned randomly. There is a total of 3 allowed questions and each robot is given an energy budget of 25% of what is needed to visit all the sites in their respectively predetermined sets. The planning results are summarized in Table 12.5. The upper half and lower half of the table show the results for the two robots, respectively. The first column shows the indices of the sites. The second column indicates whether a site is visited. The third column indicates whether a site is selected to query the human operator. The fourth and fifth columns show the performance gains associated with asking for help and visiting the sites respectively ($(p_{h,i} - p_{r,i})$ and $(\bar{p} - p_{r,i})$). The sixth column shows the motion energy costs for the sites.

For each robot's respective set of sites, it can be seen that for the sites selected for visit, their corresponding performance gains normalized by energy cost are the highest among all unqueried sites, which is consistent with Lemma 12.4. As for sites selected to query the human operator, we can see that the performance gain (5th column) of these sites obtained from asking the human are the highest among all the sites not selected for further sensing (marked by a gray color), which is consistent with Lemma 12.3.

Table 12.5 Example solution to problem (12.1) with predetermined site allocation. There are two robots, each assigned to five sites. The robots share a total of three allowed questions. Each robot is given an energy budget of 25% of what is required to visit all the sites in its own set

	Site Index	Selected for Visit	Selected for Query	Energy Cost	Performance Gain of Query	Performance Gain of Visit
Robot 1 {	1	0	1	0.6474	0.3218	0.3365
	2	1	0	0.1434	0.2917	0.3960
	3	1	0	0.0227	0.1728	0.3960
	4	1	0	0.1887	0.3511	0.3960
	5	0	1	0.5020	0.3402	0.3960
Robot 2 {	6	1	0	0.2067	0.2138	0.3960
	7	0	1	0.8360	0.3043	0.3960
	8	0	0	0.6730	0.1712	0.1460
	9	1	0	0.0168	0.3497	0.3960
	10	0	0	0.4823	0.1795	0.1460

12.4.2.3 Energy Saving

Table 12.6 shows the average amount of motion energy the robots save by using our approach when aiming to achieve a given target probability of correct classification. More specifically, the first column shows the target average probability of correct classification while the second column shows the percentage reduction in the average needed energy when using our approach as compared to the benchmark method. In the benchmark method, each robot selects the sites to visit by maximizing the total sum of variances at the sites, after which random sites are selected from the aggregated unvisited ones to query the human operator. In other words, the robots do not have the knowledge of human visual performance but know how their own performance is related to the sensing variance. In the example of Table 12.6, there is a total of four robots, each assigned to 10 sites. The robots share a total number of 10 given queries. The robots’ energy budgets are the same as each other in terms of the percentage of the total energy needed to visit all the sites in their respective sets. The noise variance of each site is randomly assigned from the interval [0.55, 4]. \bar{p} is set to 0.896. The motion energy cost to visit each site is also assigned randomly. It can be seen that the robots can reduce the energy consumption considerably by taking advantage of the knowledge of human performance and properly optimizing the collaboration accordingly. For instance, an average probability of correct classification of 0.65 is achieved with 57.14% less energy consumption.

12.4.2.4 Bandwidth Saving

We next show how our approach can also result in a considerable communication bandwidth saving by reducing the number of questions while still achieving the

Table 12.6 Energy saving as compared to the benchmark in the one-operator-multi-robot setting with preassigned sites. In this case, there are four robots, each assigned 10 sites and the robots share a total of 10 questions

Desired ave. correct classification prob.	Energy saving (in %)
0.65	57.14 %
0.7	27.78 %
0.75	27.03 %
0.8	18.75 %
0.85	10.20 %
0.9	Inf

desired performance. We consider the cases with “large bandwidth” and “zero bandwidth” as described in Sect. 12.4.1.2. Figure 12.7 compares the performance of our proposed approach with these two cases. As expected, the case of “no bandwidth” performs considerably poorly as the robots could not seek human help in classification. On the other hand, the case of “large bandwidth” performs considerably well as the robots can ask the human operator as many questions as they want to. It can be seen that our proposed approach can achieve a performance very close to this upper bound with a much less bandwidth usage. For instance, we can see that by asking only 25 questions (37.5% bandwidth reduction), the robot can achieve an average probability of correct classification of 0.817, which is only 2.4% less than the case of large bandwidth (0.835 in this case).

Table 12.7 shows the amount of bandwidth usage the robots can save by using our approach, when trying to achieve a desired average probability of correct clas-

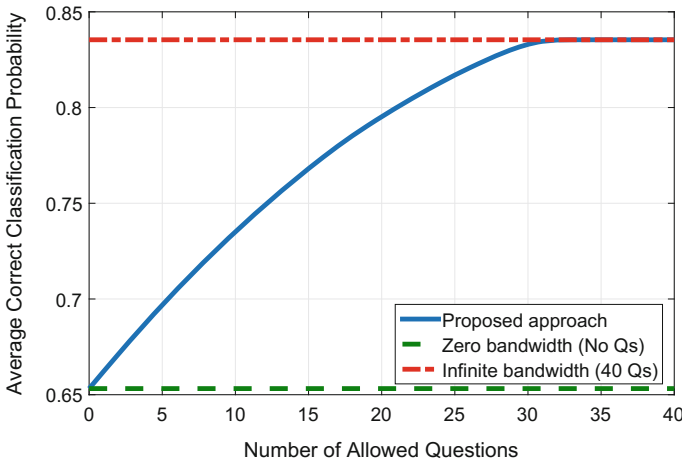


Fig. 12.7 Average probability of correct classification in a human–robot collaboration as a function of the total number of given queries. In this example, there are four robots, each assigned to 10 sites. Each robot is given a motion energy budget equal to 10% of what is needed to visit all the sites in its assigned set

Table 12.7 Bandwidth saving as compared to the benchmark in the one-operator-multi-robot setting with preassigned sites. In this case, there are four robots. Each robot is assigned to 10 sites and given 10% of what is needed to visit all the sites in its preassigned set

Desired ave. correct classification prob.	Bandwidth saving (in %)
0.65	100
0.7	33.75
0.75	22.93
0.8	14.29

sification. More specifically, the first column shows the target average probability of correct classification and the second column shows the percentage reduction of the needed bandwidth by using our approach as compared to the benchmark. In this case, each robot is given an energy budget of 10% of the total energy needed to visit all the sites in its set. It can be seen that the robot can reduce its bandwidth consumption considerably. For instance, it can achieve an average probability of correct classification of 0.7 with 33.75% less bandwidth usage.

12.4.3 Optimized Site Allocation

In this section, we conduct numerical evaluations when our approach also optimizes site allocation, as shown in problem (12.8). We first show patterns of the optimal decisions and illustrate how our approach plans the collaborative operation by showing a sample solution to problem (12.8). We then numerically demonstrate that our proposed approach can save resources significantly.

12.4.3.1 Patterns of Optimal Decisions

We solve problem (12.8) with two robots and a total of 2000 sites. There is a total of 500 given queries. The energy budget is taken as 12.5% of what is needed to visit all the sites for each robot. The noise variance of each site is randomly generated from the interval $[0.55, 4]$. \tilde{p} is set to 0.896. The motion energy cost to visit each site is also assigned randomly for each robot. The pattern of optimal decisions in terms of asking for human help, visiting a site and relying on the initial sensing for any one of the two robots in this scenario is very similar to those shown in Figs. 12.3 and 12.5.

Here, we show how the optimal decisions are related to the motion energy costs of visiting the sites for the two robots. Figures 12.8 and 12.9 show when the robots will visit a site, when they will query the human operator and when they will rely on the initial sensing. Green disks represent asking for human help, red diamonds indicate that the site is visited by robot 1, yellow triangles indicate that the site is visited by robot 2, and blue squares represent the decision of relying on the initial

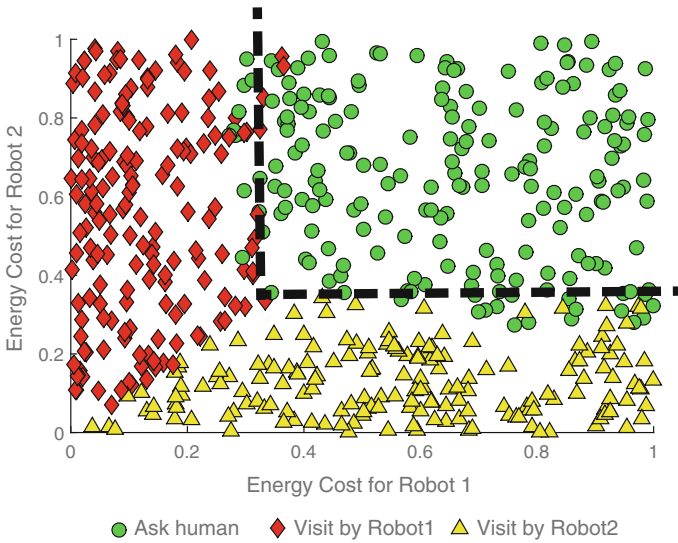


Fig. 12.8 An example of the optimal decisions with two robots with 2000 sites, 500 questions. Each robot's energy budget is 12.5% of the total energy needed for it to visit all the sites

sensing. It can be seen that the two robots select sites that do not require too much motion energy to visit. Note that it may cost the robots different amount of motion energy to visit the same site. For a site that is costly to visit for both robots (sites that reside in the top-right region of Figs. 12.8 and 12.9), the robots will either query the human operator or rely on the initial sensing depending on the noise variance of the site. We note that in Fig. 12.9, there is a number of sites for which the robots will rely on the initial sensing even though the costs of visiting them is not high for at least one of the robots. This is because the noise variances associated with these sites are already low, eliminating the need for further sensing.

12.4.3.2 Example Solution

In this section, we show a sample numerical solution to problem (12.8). We consider the case with two robots and 10 sites. The noise variance of each site is randomly assigned from the interval $[0.55, 4]$. \bar{p} is set to 0.896. The motion energy cost to visit each site is also assigned randomly for each robot. There is a total of two allowed questions and each robot is given 12.5% of what is needed for it to visit all the sites. The planning results are summarized in Table 12.8. The first column shows the indices of the sites. The second column indicates whether a site is visited by robot 1 and the third column indicates whether a site is visited by robot 2. The fourth column indicates whether a site is selected to query the human operator. The fifth and sixth columns show the motion energy costs for visiting the sites for robot 1 and

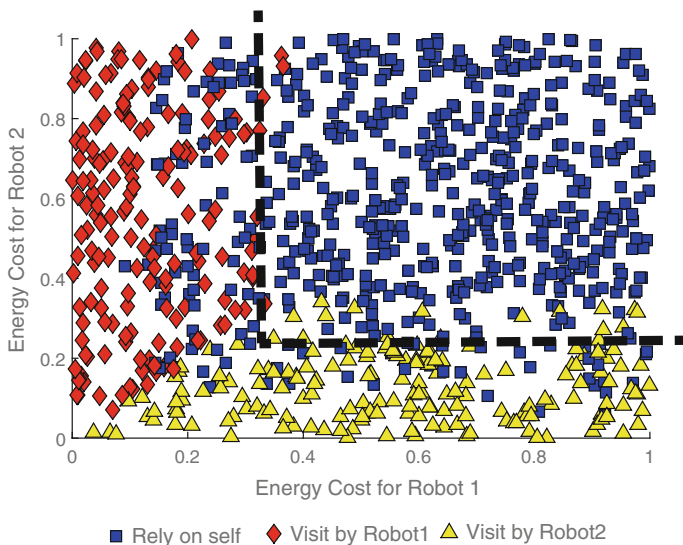


Fig. 12.9 An example of the optimal decisions with two robots with 2000 sites, 500 questions and each robot’s energy budget is 12.5% of the total energy needed for it to visit all the sites

Table 12.8 An example solution to problem (12.8) with an optimized site allocation. There are two robots and 10 sites. There is a total of two allowed questions and each robot is given 12.5% of what is required for it to visit all the sites

Site index	Visited by robot 1	Visited by robot 2	Selected for query	Energy cost for robot 1	Energy cost for robot 2	Performance gain of query	Performance gain of visit
1	0	0	0	0.9469	0.9705	0.2879	0.3960
2	0	0	1	0.8077	0.8802	0.3113	0.3960
3	1	0	0	0.1245	0.6473	0.1963	0.2028
4	0	1	0	0.9662	0.0892	0.1885	0.3960
5	0	0	0	0.6030	0.6419	0.2852	0.3960
6	0	1	0	0.6766	0.0732	0.3390	0.3960
7	0	0	0	0.2427	0.2997	0.1695	0.1460
8	0	0	1	0.9348	0.6253	0.3381	0.3960
9	0	1	0	0.5331	0.0288	0.1755	0.1460
10	1	0	0	0.0088	0.1586	0.1807	0.1860

robot 2, respectively. The seventh and eighth columns show the performance gains associated with asking for human help and visiting the sites respectively ($(\tilde{p}_{h,i} - \tilde{p}_{r,i})$ and $(\tilde{p} - \tilde{p}_{r,i})$).

We can see that if a robot visits a particular site, the performance gain from visit normalized by this robot’s energy cost associated with this site is greater than or

equal to that of any other unvisited site, which is consistent with Lemma 12.7. We note that although the performance gain achievable from visiting site 1 is larger than those of sites 3, 9, and 10, site 1 is not visited while the latter three are visited. This is because the motion energy required to visit site 1 is too high for both robots. As for the sites selected for query, it can be seen that these sites have a significantly larger performance gain from asking for human help as compared to any other unvisited site, which is consistent with Lemma 12.6.

12.4.3.3 Energy Saving

Table 12.9 shows the amount of average motion energy the robots save by using our approach when aiming to achieve a desired probability of correct classification. The first column shows the desired average probability of correct classification while the second column shows the percentage reduction of the needed energy by using our proposed approach as compared to a benchmark method similar to the one described in the previous section. In the benchmark method, the robots select the sites to visit by maximizing the total sum of sensing variances under the given energy budgets, after which random sites are selected from the remaining ones to query the human operator. In this case, there is a total of four robots with a total of 40 sites. The robots are given 10 allowed queries. The robots' energy budgets are the same as each other in terms of the percentage of the total energy needed to visit all the sites. The noise variance of each site is randomly assigned from the interval $[0.55, 4]$. \bar{p} is set to 0.896. The motion energy cost to visit each site is also assigned randomly for each robot. It can be seen that the robots can reduce their average energy consumption considerably by properly taking advantage of the knowledge of human visual performance. For instance, an average probability of correct classification of 0.7 can be achieved with a 40.00% less energy consumption.

Table 12.9 Energy saving as compared to the case of no proper collaboration in the one-operator-multi-robot setting with an optimized site allocation. In this case, there are four robots with 40 sites and there is a total of 10 questions

Desired ave. correct classification prob.	Energy saving (in %)
0.65	75.00 %
0.7	40.00 %
0.75	25.00 %
0.8	18.18 %
0.85	10.53 %
0.9	Inf

12.4.3.4 Bandwidth Saving

We next show how our approach can also result in a considerable communication bandwidth saving by reducing the number of questions needed while still providing a good performance. We consider the cases of “large bandwidth” and “zero bandwidth” as described in Sect. 12.4.1.2. Figure 12.10 compares the performance of our proposed approach with these two cases. We can see that by asking only 20 questions (50% bandwidth reduction), the robot can achieve an average probability of correct classification of 0.857, which is only 0.8% less than the case of large bandwidth (0.864 in this case).

Table 12.10 shows the amount of bandwidth that the robots can save by using our approach, when trying to achieve a desired average probability of correct classification. The first column shows the target average probability of correct classification and the second column shows the percentage reduction of the needed bandwidth by using our proposed approach as compared to the benchmark. In this case, each robot is given an energy budget of 10% of the total energy needed for it to visit all the sites. It can be seen that by properly designing the collaboration, we can reduce the bandwidth consumption considerably. For instance, an average probability of correct classification of 0.75 can be achieved with a 48.57% less bandwidth usage.

Overall, we can see that by using our proposed collaboration approach, we can reduce the motion energy and bandwidth consumptions considerably.

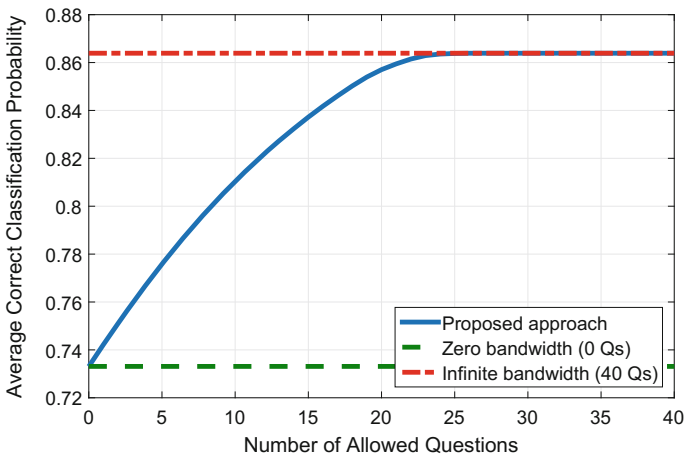


Fig. 12.10 Average probability of correct classification in the one-operator-multi-robot collaboration as a function of the total number of given queries. In this example, there are four robots with 40 sites and each robot’s motion energy budget is 10% of what is needed for it to visit all the sites

Table 12.10 Bandwidth saving as compared to the benchmark in the one-operator-multi-robot setting with an optimized site allocation. In this case, there are four robots with 40 sites and each robot’s motion energy budget is 10% of what is needed for it to visit all the sites

Desired ave. correct classification prob.	Bandwidth saving (in %)
0.75	48.57 %
0.8	25.23 %
0.85	Inf

12.5 Conclusions

In this chapter, we extended our previously proposed paradigm for human–robot collaboration, namely, “when to ask for human’s help”, to the case of multiple robots. More specifically, we considered a robotic field exploration and target classification task where a number of robots have a limited communication with a remote human operator and constrained motion energy budgets. The visual performance of the human operator, however, is not perfect and is given via a probabilistic modeling from [4]. We started with the case where the sites, which contain the objects to be classified, are preassigned to the robots in order to understand optimum allocation of other resources. We then extended our analysis to further include the optimization of site allocation. Simulation results confirm that considerable resource savings can be achieved using our proposed approach. Overall, our framework allows the robots to collaboratively and optimally decide on when to ask humans for help, when to rely on the initial sensing, and when to gather more information from the field.

Acknowledgements This work was supported in part by NSF NeTS award #1321171 and NSF RI award #1619376.

References

1. Boyd S, Vandenberghe L (2009) *Convex Optimization*. Cambridge university press, Cambridge
2. Branson S, Wah C, Schroff F, Babenko B, Welinder P, Perona P, Belongie S (2010) Visual recognition with humans in the loop. In: *Proceedings of the European conference on computer vision*, pp 438–451
3. Burke J, Murphy R, Covert M, Riddle D (2004) Moonlight in miami: field study of human-robot interaction in the context of an urban search and rescue disaster response training exercise. *Hum-Comput Interact* 19(1–2):85–116
4. Cai H, Mostofi Y (2015) To ask or not to ask: a foundation for the optimization of human-robot collaborations. In: *Proceedings of the American control conference*, pp 440–446
5. Cai H, Mostofi Y (2016) Asking for help with the right question by predicting human performance. In: *Proceedings of robotics: science and systems*
6. Cai H, Mostofi Y (2016) A human-robot collaborative traveling salesman problem: robotic site inspection with human assistance. In: *Proceedings of the American control conference*

7. Cao M, Stewart A, Leonard N (2008) Integrating human and robot decision-making dynamics with feedback: models and convergence analysis. In: Proceedings of the IEEE conference on decision and control, pp 1127–1132
8. Chipalkatty R (2012) Human-in-the-loop control for cooperative human-robot tasks. Ph.D. thesis, Georgia Institute of Technology
9. Dantzig GB (1957) Discrete-variable extremum problems. *Oper Res* 5(2):266–288
10. Dias MB, Kannan B, Browning B, Jones E, Argall B, Dias MF, Zinck M, Veloso M, Stentz A (2008) Sliding autonomy for peer-to-peer human-robot teams. In: Proceedings of the international conference on intelligent autonomous systems, pp 332–341
11. Martello S, Toth P (1990) Knapsack problems: algorithms and computer implementations. Wiley, New York
12. Meriçli Ç, Veloso M, Akin H (2011) Task refinement for autonomous robots using complementary corrective human feedback. *Int J Adv Robot Syst* 8(2):68
13. Srivastava V (2012) Stochastic search and surveillance strategies for mixed human-robot teams. Ph.D. thesis, University of California, Santa Barbara
14. Stewart A, Cao M, Nedic A, Tomlin D, Leonard N (2012) Towards human-robot teams: model-based analysis of human decision making in two-alternative choice tasks with social feedback. *Proc IEEE* 100(3):751–775
15. Toris R, Suay H, Chernova S (2012) A practical comparison of three robot learning from demonstration algorithms. In: Proceedings of the ACM/IEEE International Conference on Human-Robot Interaction, pp 261–262